Desalination and Water Treatment
www.deswater.com
doi: 10.5004/dwt.2022.28075

247 (2022) 281–293
January

Investigation of adsorption performances of green walnut hulls for the removal of methylene blue

Yasemin İşlek Coşkun

Department of Chemistry, Faculty of Science, Ege University, 35100 Bornova, Izmir, Turkey, Tel. +90(232)3112389; Fax: +90(232)3888294; email: yasemin.islek@ege.edu.tr, ORCID ID: 0000-0003-3207-4381

Received 7 October 2021; Accepted 19 December 2021

ABSTRACT

Green walnut hulls are agricultural wastes released in vast amounts in Turkey. In this study, green walnut hulls were used, without complex preparation, for the adsorption of methylene blue from an aqueous medium. The influence of the optimum pH, initial dye concentration, adsorbent dose, and agitation time on adsorption was explored. Optimal experimental conditions were detected to be pH 10, 0.5 g/L of the adsorbent dose with 1,440 min of agitation time. The experimental data complied with the Langmuir isotherm model, indicating chemisorption. According to this model, the adsorbent capacity was 1,000 mg/g, and this process followed the pseudo-second-order kinetic model. According to the thermodynamic investigation, the adsorption process of methylene blue on green walnut hulls was exothermic, feasible, and spontaneous. Desorption studies and analytical applications were also executed. The usage of green walnut hulls ensures not only reduced green walnut hulls wastes for environmental safety, but also provides a cheap and abundant adsorbent for dye removal.

Keywords: Adsorption; Green walnut hulls; Methylene blue

1. Introduction

A major problem of today is rapidly increasing environmental pollution. In this case, the impact of the wastewater released from factories to rivers, lakes, and seas without treatment is still quite high. Environment pollution led by the paint industry is prominent because it causes serious damage to aqueous vegetation, microorganisms, and human beings [1–3]. Methylene blue (MB) is a basic dye utilized in paper, textile, carpet, and leather industries as well as in printing and some fish farms. Exposure to MB in high doses may cause nausea, headaches, shortness of breath, vomiting, confusion, and high blood pressure [2,4–7]. Due to the presence of nitrogen in its complex aromatic structure, it possesses highly mutagenic, teratogenic, chromosomal fractures, and carcinogenic properties [8]. In addition, artificial dyes have been linked to major adverse effects, including hyperactivity in children, cancer, and allergies in both adults and children [9]. Therefore, it is extremely beneficial to remove MB from water.

Considering the high permanence of dyes in nature and how they affect water quality even at low concentrations, removing them from wastewater has become very important. Wastewater treatment can be carried out by biological, physical, and chemical processes; nonetheless, these methods generally have many disadvantages. Biological procedure needs a great deal of space, is sensitive to daily changes, allows for easy exposure to chemicals, and has a rigid design. Chemical and physical methods including ion-exchange, coagulation, membrane separation, flocculation, oxidation, and adsorption, are usually expensive, require high energy, and are suitable for limited areas. However, physical methods for dye removal are mostly used due to their simplicity and effectiveness [10].

* Corresponding author.

Adsorption offers superior features to the other traditional methods mentioned above regarding efficiency, practicality, ecological benefits, easier application methods, and selectivity [7,11,12]. Furthermore, the adsorption processes can impede the occurrence of by-products resulting from oxidation or the decomposition of dyes [13]. The approach is especially effective for dye sequestration because it allows the molecule to be securely recovered without fragmenting or distorting its bulky structure [14]. Because the efficiency of adsorption is totally dependent on the nature of the adsorbent, researchers are always on the lookout for a material that is both efficient and cost-effective. It is accepted that the adsorbent's reusability is the most important aspect impacting the adsorption process' efficiency. It is usually desirable to have a durable material that can withstand several adsorption/desorption cycles and remains unaffected even after extended use [15,16].

Agricultural by-products and agricultural wastes are often preferred due to their effectiveness as well as their cheap and easily accessible nature. In addition, the usage of agricultural wastes or by-products as adsorbents could help to reduce the amount of waste. Besides, agricultural waste materials can also be used as alternative process adsorbents in dye removal. Banana peel waste [7], corn cobs [4], parsley stalks, cucumber peels, watermelon seed hulls [6], waste of citrus limetta peel [2], Lathyrus sativus husk [17], macadamia nutshells [18], and cashew nutshells [19] are some of the agricultural-based adsorbents discussed in the literature. In Turkey, the walnut is a product that grows in abundance. The husk or hull is the outer greenish layer and has been used in limited studies [20]. It is an abundant agricultural waste [21]. The green walnut hull was reported to have a large surface area, a porous structure that provides a higher capacity, and it is easy to obtain [22]. Çelekli et al. [21] researched Lanaset Red G removal using walnut husk and reported the kinetic model of pseudo-second-order is valid. Basic Red 46 was also removed by a walnut husk with a maximum capacity of 66.45 mg/g [23]. The walnut hull was employed for Cu(II) adsorption and yielded a Langmuir capacity of 3.52 mg/g for the Cu(II) [24]. Cr(VI) removal with walnut hull was successfully performed with a removal efficiency of 97.3% [25]. Phenol in water was eliminated by a walnut green husk at pH 4 [22]. Dalali and Hagghi [26] used walnut green husk to eliminate Cd(II) from aqueous solutions. It was reported that sorption adhered to both the Freundlich and Langmuir models. However, no further studies can be found in the literature. From this point of view, this study is the first on MB removal using green walnut hulls as adsorbents.

The usage of green walnut hulls ensures not only reduced walnut waste for environmental safety, but also provides a cheap and abundant adsorbent for MB removal. In this research, the influence of pH, agitation time, adsorbent dose, temperature, and initial MB concentration was appraised, in addition to equilibrium, thermodynamic, and kinetic models.

2. Materials and methods

Hydrochloric acid (HCl), ethanol, sodium hydroxide (NaOH), nitric acid (HNO_3), sodium chloride (NaCl), acetone and methylene blue (CI. 52015) (molecular weight 319.85 g/mol, λ_{max} 663 nm) (MB) were purchased from Merck. The MB stock solution (1,000 mg/L) was prepared by the dissolution of the aliquot amount of MB. The model solutions and standards of MB were prepared daily. HCl (1 mol/L), HNO_3 (1 mol/L), NaCl (1 mol/L), NaOH (2 mol/L), ethanol, and acetone were used for the desorption studies.

A pH meter was utilized for adjusting the pH of the solutions (Mettler Toledo Five Go FG-2). The adsorption studies were executed by using a vibration water bath (Nuve ST-402) and an orbital shaker at 350 rpm (Biosan OS-10). The absorption measurements for the MB were carried out using a PG Instruments TG 80+ model UV-Vis spectrophotometer (double beam) at 663 nm. The FT-IR spectroscopy (Fourier-transform infrared spectroscopy) examinations of the green walnut hulls was performed between 4,000 and 400 cm^{-1} (Perkin Elmer 100). The scanning electron microscopy (SEM) analysis for the surface morphology and energy-dispersive X-ray spectroscopy (EDX) was carried out by using a Thermo Scientific Apreo S Lo Vac. The Brunauer, Emmet, and Teller (BET) analysis was performed using a Quantachrome Autosorb-IQ2 model gas sorption analyzer. The elemental analyses were actualized by using a Leco Truspecmicro elemental analyzer. The pH_{pzc} (point of zero charge) value of the green walnut hulls was determined according to the following method. First, 25 mL of 0.01 mol/L NaCl solution in which the solution pH was set to 2–11 was added onto 10 mg of adsorbents. The solutions were agitated for 1440 min. Finally, the final pH of the solutions was assessed. The plot of ΔpH ($pH_{initial}$–pH_{final}) vs. $pH_{initial}$ was formed.

The green walnut hulls were provided by a local manufacturer. First, the green walnut hulls were peeled and broken into smaller pieces. These pieces were treated with deionized water several times and then, shaken with deionized water for one night. Afterwards, to remove the green-brown color, the hulls were shaken with ethanol. Finally, the hulls were dried at 75°C in an oven for 2 d and then sieved.

Optimization studies were executed in batch mode and triplicate. 20 mL of solution containing 20 mg/L of MB was used. The optimum pH was investigated in the range of pH 2–11, while the optimum adsorbent mass was examined for 10, 20, 30, and 60 mg. HCl and NaOH were used for setting the initial pH of the MB. Ten mg of the green walnut hulls were weighted and 20 mL 20 mg/L of MB solution at a pH 2–11 range was added onto the adsorbent. Then, they were agitated for 1440 min using an orbital shaker at 298 K. Afterwards, the supernatant was separated by filter paper. The agitation time and kinetic models were studied for 5, 15, 30, 60, 120, 600, and 1,440 min using 10 mg of the adsorbent amount, 20 mL 20 mg/L of MB concentration at pH 10. Unless otherwise stated, the optimization studies were performed for 1,440 min. The initial MB concentration and adsorption isotherms were investigated for 10, 25, 50, 100, 400, 800, and 1,000 mg/L. The effect of the temperature and thermodynamic models were studied at 291, 303, 333, and 353 K. The supernatant was taken and acidified by HCl before measurement. Subsequently, the unadsorbed MB concentration was determined at 663 nm. To calculate the MB adsorption efficiency (R, %), the equation depicted below was used.

$$\% R = \frac{C_i - C_e}{C_i} \times 100 \quad (1)$$

The initial and at equilibrium MB concentrations are C_i (mg/L) and C_e (mg/L), respectively. The adsorbed amounts of MB by the green walnut hulls adsorbent is shown by the following equation.

$$q = \frac{(C_i - C_e)V}{m} \quad (2)$$

where q is the amount of the adsorbed MB (mg/g), C_i and C_e are the initial and equilibrium MB concentration (mg/L), V is the volume of MB (L), and m is the amount of the green walnut hulls (g).

3. Results and discussion

3.1. Characterization of the green walnut hulls

Green walnut hulls have a complex structure consisting of tannins, naphthoquinones, glycosides, naphthalenones, α-tetralones, hydroxybenzoic acids, hydroxycinnamic acids, flavonoids, diarylheptanoids, lignin, cellulose, and hemicellulose [20,27]. The cellulose and hemicellulose include various functional groups which have an affinity to heavy metal and dye molecules. For instance, hydroxyl and carboxyl functional groups are found in the cellulose, and hydroxyl can form intermolecular hydrogen bonds [28,29]. Moreover, Zhu et al. [30] reported these structures have polar functional groups such as carboxyl groups and phenolic hydroxyl as chemical bonding agents which lead to chemical sorption.

The Fourier-transform infrared spectrum of the green walnut hulls before and after MB adsorption is given in Fig. 1. The spectra were registered from 4,000–400 cm^{-1} preparing KBr pellets. The broad bands at 3,425 and 3,333 cm^{-1} are attributed to the –OH stretching vibration of the hydroxyl groups and $–NH_2$ groups [28,31]. The peaks at 2,919; 2,851 and 2,850 cm^{-1} for two adsorbents indicate C–H stretching of the methylene groups. Although no significant shifts were observed for these bands, the band intensities were seen to increase after the adsorption of MB. The bands at 1,737 and 1,731 cm^{-1} pointed out C=O stretching [31,32]. An apparent shift of C=O stretching in the amide groups (amide band 1) or carboxyl occurred at 1,622 to 1,602 cm^{-1}, and severe changes at peak intensities were also observed. The shifting from 1,373 to 1,390 cm^{-1} and 1,318 to 1,328 cm^{-1} indicated O–H bending and C–N stretching. The increase in the peak intensities was barely seen, which could be a result of the adsorption of the MB on the green walnut hulls. The band shifts from 1,249 to 1,236 cm^{-1} could be associated with the C–O–C asymmetrical stretching of hemicellulose, cellulose, and lignin [21,33]. The peaks at 1,067 and 1,031 cm^{-1} could be attributed to the C–O–C stretching vibrations in the phenols, alcohols, ester or ether group in cellulose [32–35]. Godini et al. [22] reported similar peaks for bare green walnut hulls as those found in the current study.

In brief, it was thought that the main functional group contributing to the adsorption process was the carboxyl group. Li et al. [31] mentioned that the power of electrostatic interactions is not sufficient to alter the peaks of the functional groups on the adsorbent surface. This shifting could result from complex processes between the ionizable functional groups and the MB molecule.

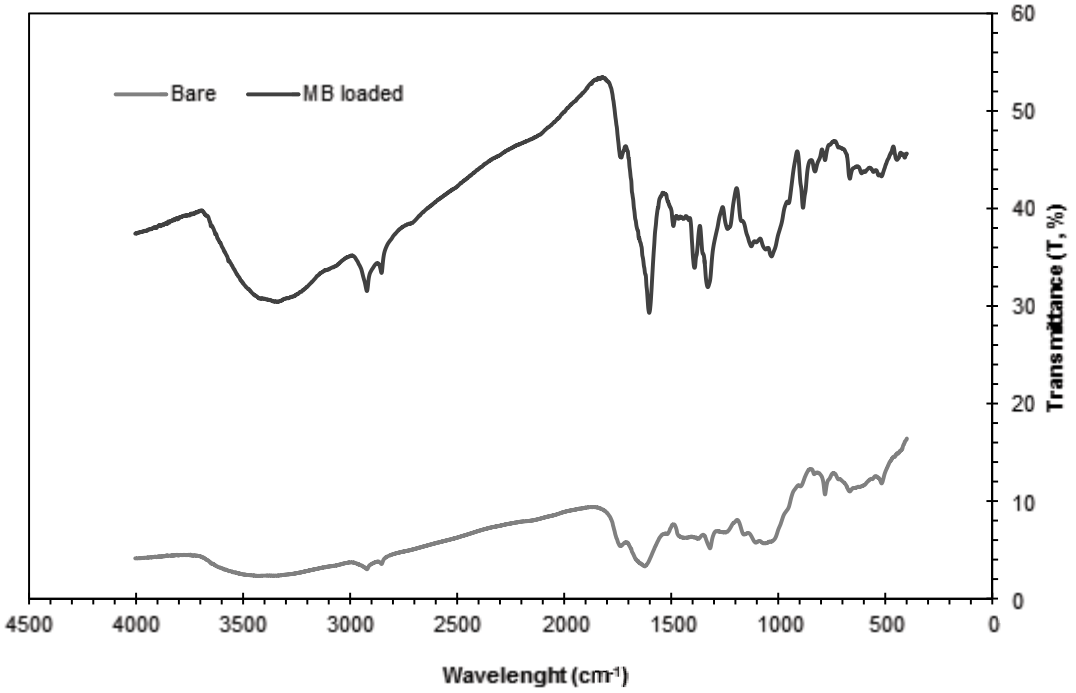

Fig. 1. Fourier-transform infrared spectrum of bare and MB loaded green walnut hulls.

SEM was performed for revealing the surface morphology of the green walnut hulls. The elemental analysis of the green walnut hulls' surface was carried out by EDX. The SEM and the EDX images are displayed in Fig. 2. A structure in which small plates are placed vertically stood out when the bare adsorbent was examined. Moreover, after the magnification factor increased, it was understood that there were many indentations and protrusions on the surfaces of these plates. The existence of these structures also increased the surface area. In the EDX images, the peaks belonging to N and S atoms observed after the adsorption could be evidence of the adsorption of the MB molecule. The BET results revealed that the surface area of the adsorbent was 8.372 m^2/g, the total pore volume $1.7075 \cdot 10^{-3}$ cm^3/g, and the average pore radius $0.4079 \cdot 10^{1}$ Å. According to the elemental analyses,

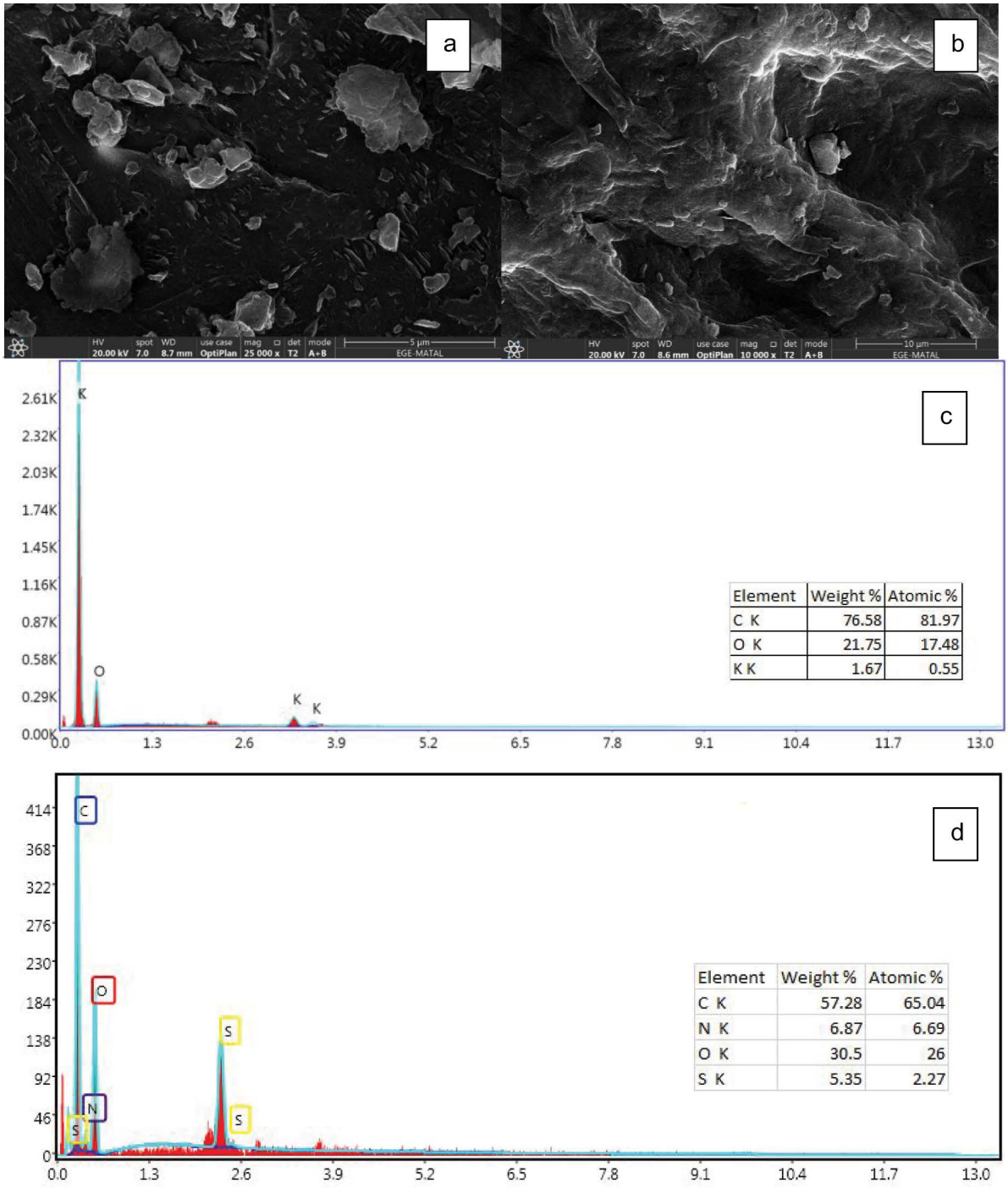

Fig. 2. SEM and EDX images of the green walnut hulls before (a, c) and after (b, d) MB adsorption.

the green walnut hulls adsorbent consisted of 1.08% N, 43.96% C, 5.55% H, and the value of S was not detectable.

The pH_{pzc} value of the green walnut hulls was determined as 7.2. If pH_{pzc} was higher than solution pH, the green walnut hulls' surface became positive and repelled the positively charged species. The pH values above the pH_{pzc}, meant that the surface charge of the green walnut hulls became negative and attracted the positively charged species.

3.2. Adsorption performances at different pH levels

The solution's pH is the most critical criterion affecting the adsorption performances by altering the functional groups of the analyte and adsorbent, and the surface charge. The adsorption performances were investigated between the pH values of 2 and 11. The calculated removal efficiencies are displayed in Fig. 3. A maximum adsorption efficiency was reached at pH 10 with 92.97 ± 0.21%. As seen in Fig. 3, the removal efficiencies were increased as the pH was increased. Before the pH_{pzc} value, the high amount of the competitive H^+ in solutions make the active sites of the green walnut hulls more positive (protonation of the functional groups such as $–OH_2^+$, protonation of carboxylic acid groups). Therefore, electrostatic repulsion occurs between the positively charged green walnut hulls surface and cationic dye, and MB, resulting in decreased removal efficiencies. After pH_{pzc}, the removal efficiencies of the MB increased due to the electrostatic interaction between negatively charged active sites of the adsorbent (deprotonated surface) and positively charged MB molecules [36]. After the pH_{pzc} value, the removal efficiencies reached the highest value. Hence, the presence of electrostatic interactions could be seen between the green walnut hulls and the MB molecules [28,37]. Rashid et al. [38] also reported the presence of the electrostatic interactions between MB and a pumpkin peel activated carbon adsorbent.

As mentioned above, electrostatic interactions were thought to be present. As the electrostatic attraction between the negative charged surface of the adsorbent and positively charged MB increased at higher pHs, the rate of the adsorption of the cationic dye also increased. The optimum pH value was compatible with the earlier studies in the literature for MB removal [38–40].

3.3. Adsorption performances in the presence of ionic strength

Salts are used in enormous quantities during the dyeing process. The effect of ionic strength on the removal of MB was investigated by using 0, 0.05, 0.25, and 1% of NaCl as a representative background impurity. The mentioned amount of the NaCl was added to the 20 mg/L of MB solution. The results are depicted in Fig. 4. The removal efficiencies decrease while the ionic strength of the solution increases. It has been reported in previous studies that this trend could be the result of the weakening electrostatic attraction between the analyte and the adsorbent due to the presence of NaCl [41,42]. Besides, the presence of sodium ion could reduce the surface charge of the adsorbent and leads to the aggregation of the adsorbent [43,44]. Similar results were reported in the literature [36,43,45].

3.4. Adsorption performances in different amount of adsorbent

The adsorption performances of the green walnut hulls for the adsorbent amounts in the range of 5–60 mg were examined. The results are depicted in Fig. 5. The calculated values were 91.90 ± 0.031%, 93.44 ± 0.79%, 91.03 ± 0.19%, 90.27 ± 0.17%, 91.75 ± 0.01% for 5, 10, 20, 30, and 60 mg of adsorbent amount, respectively. Although the removal efficiencies did not change significantly, the 10 mg of the adsorbent amount (0.5 g/L of dose) was the highest value and thus was selected for further studies. That trend might be the result of a high number of active sites, or pores that approve effortless adsorption [24]. Markovic et al. [46] calculated the optimum dose of the raw peach shell particles to be 4 g/L for 20 mg/L of the MB removal. Ng et al. [33] used 0.05 g of rice husk and oil palm empty fruit bunch for the removal of the MB solution

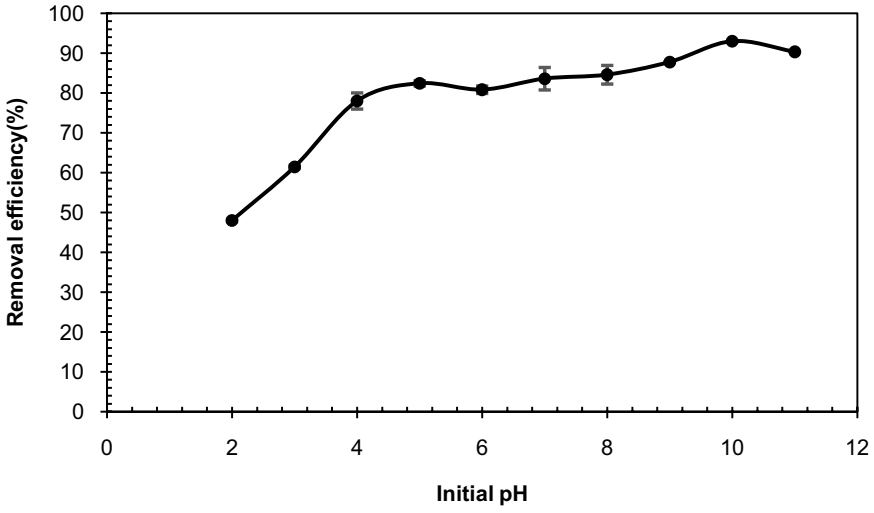

Fig. 3. The adsorption performances at different initial solution pH (Experimental conditions: initial pH range: 2–11, adsorbent amount: 10 mg, initial MB concentration: 20 mg/L, agitation time: 1,440 min, volume of the solution: 20 mL).

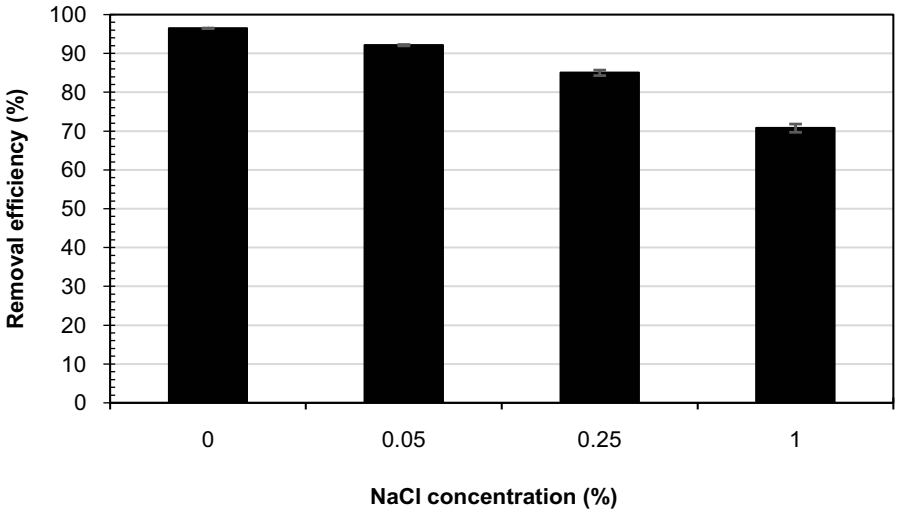

Fig. 4. Adsorption performances in the presence of ionic strength (Experimental conditions: initial pH: 10, adsorbent amount: 10 mg, initial MB concentration: 20 mg/L, agitation time: 1,440 min, volume of the solution: 20 mL, NaCl concentration 0–1%).

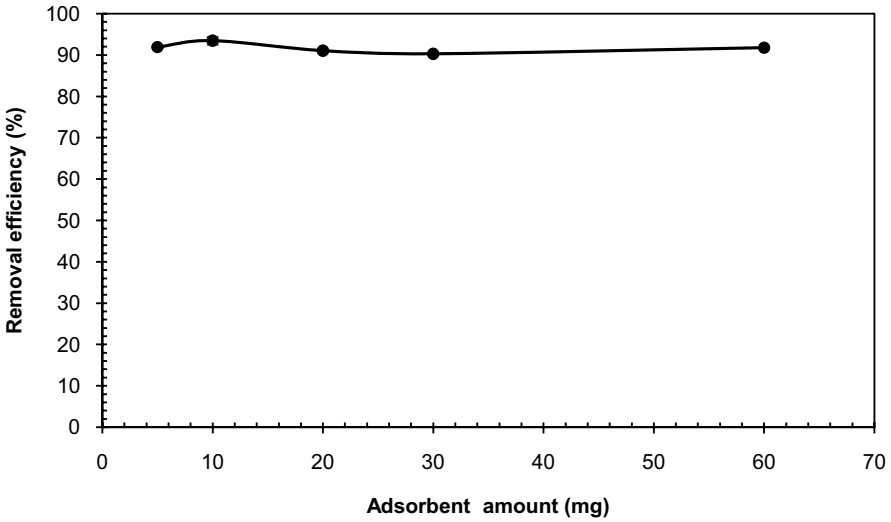

Fig. 5. The adsorption performances in different adsorbent amount (Experimental conditions: initial pH: 10, adsorbent amount range: 5–60 mg, initial MB concentration: 20 mg/L, agitation time: 1,440 min, volume of the solution: 20 mL).

concentration ranging from 4–12 mg/L. It was reported that the optimum adsorbent dose of chemically transformed soya waste was 2 g/L for the removal of 50 mg/L of MB concentration [47].

3.5. Equilibrium studies and investigation of initial concentration

Adsorption isotherms help to comprehend the distributions of molecules between an adsorbent and adsorbate at the equilibrium time. Adsorption isotherms associate the amount of analyte absorbed by the adsorbent with the concentration of analyte remaining in the solution after the equilibrium is reached. Furthermore, isotherm models allow for the evaluation of the adsorption mechanism. The most used isotherm models, being the Langmuir, Freundlich, and Dubinin–Radushkevich (D-R) models, were used in the current study for this evaluation. The Langmuir model assumes a homogeneous surface with a finite number of adsorption sites, with adsorption taking place at a monolayer in nature, and expects chemisorption. This model confirms that there is no interaction between the adsorbed molecules [46], whereas the Freundlich model suggests a heterogeneous surface, multilayer adsorption, and the presence of interactions between the adsorbed molecules [6,47]. The D-R isotherm model is more general than the Langmuir model, suggesting that the surface is not homogeneous and that the energy of the surface is differentiated during the adsorption [30]. The equations of the Langmuir, Freundlich, and D-R isotherm models are given in Table 1.

The isotherm models were investigated in experimental conditions using pH 10, 10 mg of the adsorbent amount, 20 mL of solution volume, 1,440 min of agitation time, and

Table 1
Calculated isotherm values of the Langmuir, Freundlich, and D-R models for MB adsorption on the green walnut hulls

Langmuir isotherm model		
$\frac{C_e}{q_e}=\left(\frac{1}{Q_{max}}\right)C_e+\frac{1}{bQ_{max}}$	Q_{max} (mg/g)	1,000
	b (L/mg)	0.03533
$q_e=\frac{C_e q_m K_L}{1+C_e K_L}$	R^2	0.994
	Separation factor (R_L)	0.531–0.028
Freundlich isotherm model		
$\log q_e=\log K+\frac{1}{n}\log C_e$	$1/n$	0.4537
$q_e=K_F C_e^{1/n}$	K (mg/g)(L/mg)$^{1/n}$	66.97
	R^2	0.9593
D-R isotherm model		
$\ln Q=\ln Q_m-k\varepsilon^2$	E (kJ/mol)	11.32
	Q_m (mol/g)	0.0088
$E=\left(2k\right)^{-0.5}$	k (mol^2/kJ^2)	0.0039
	R^2	0.9743

q_e: amount of adsorbed MB/amount of adsorbent (mg/g); C_e: equilibrium concentration of the solution (mg/L); Q_{max}: monolayer adsorption capacity of Langmuir isotherm model (mg/g); b: Langmuir constant (L/mg), $1/n$: dimensionless Freundlich constant for the intensity of the adsorbent; K: Freundlich constant ((mg/g)(L/mg)$^{1/n}$); ε: Polanyi potential ($RT\ln(1+1/C_e)$); T: absolute temperature (K); Q: amount of dye adsorbed per unit weight of adsorbent (mol/g); R: gas constant (kJ/mol K); Q_m: adsorption capacity (mol/g); k: factor associated to adsorption energy (mol^2/kJ^2).

25, 50, 100, 200, 400, 800 and 1,000 mg/L of the initial MB concentration. The isotherm values are presented in Fig. 6 and Table 1.

It was found that by increasing the concentration of MB from 25 to 1,000 mg/L, the removal efficiency was reduced from 96.8% to 47.3%. This was because of the limited number of active sites saturated in high concentrations of dye. Similar results were also obtained by Nasseh et al. [48].

Considering the maximum coefficients of correlation (R^2), the experimental datum follows the Langmuir isotherm expressing monolayer and homogeneous adsorption. According to this model, the adsorption of MB on the green walnut hulls was chemisorption-based. Meanwhile, in Fig. 6e, it was clearly seen that the Langmuir model was more satisfactorily fitted to the experimental data than that of the Freundlich model. The Langmuir isotherm indicated that when the concentration rises to a saturation point, the amount of methylene blue adsorbed increases. Increasing the methylene blue concentration beyond this point will not result in any additional increases. Adsorption increases with increasing methylene blue concentration if available sites exist. A further increase in the methylene blue concentration will not enhance the quantity of methylene blue on the adsorbent once all the sites have been occupied. $1/n$ value shows the heterogeneity of the surface, where if the values are closer to zero, the surface becomes more heterogeneous, and if the values are lower than 1, a normal Langmuir isotherm is indicated [49]. As seen in Table 1, the $1/n$ value (0.4537) was below 1, and the adsorption obeyed the normal Langmuir isotherm model. Besides, the separation factor (R_L) value indicates whether the adsorption is favorable or not. The adsorption is favorable if the R_L value is in the range of 0–1, then, a value above 1 indicated unfavorable adsorption. If the R_L is 1, shows the linear adsorption and an R_L equal to 0 shows irreversible adsorption [6]. As indicated in Table 1, since the R_L values lay mostly in the range of 0.531–0.028, adsorption was favorable.

The mean free energy of the adsorption (E) can be calculated from the related equation in Table 1. If the value of E is between 8 and 16 kJ/mol, the adsorption process is chemical sorption or ion exchange, and if it is less than 8 kJ/mol, the adsorption process is physical [30]. As tabulated in Table 1, the E value was 11.32 kJ/mol, showing that the chemisorption or ion exchange was valid for the adsorption of the MB on the green walnut hulls. The biosorption of the MB by cucumber peels and watermelon seed hulls [6], the removal of MB with pumpkin peel activated carbon adsorbent [38], and isotherm data of silica coated soya waste [47], all conform to the Langmuir model. Conversely, the application of raw peach shells for the MB removal indicated that the

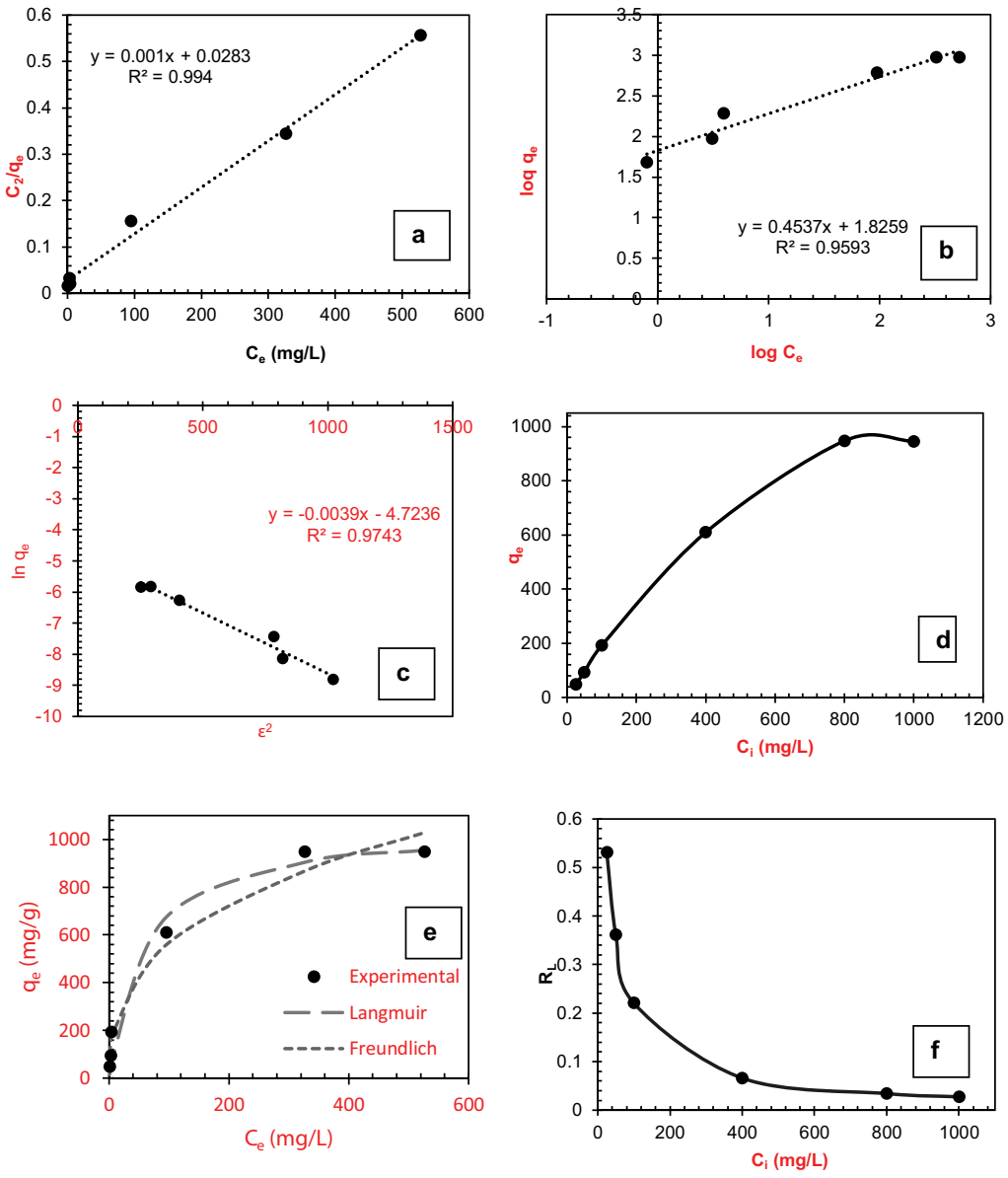

Fig. 6. Graphs of isotherm models, (a) Langmuir, (b) Freundlich, (c) D-R isotherm models, (d) adsorption capacity vs. initial MB concentration, (e) q_e values vs. C_e, and (f) values of R_L vs. C_i (Experimental conditions: initial pH: 10, adsorbent amount: 10 mg, initial MB concentration: 25–1,000 mg/L, agitation time: 1,440 min, volume of the solution: 20 mL).

mechanism of biosorption agreed with the Freundlich and Brunauer-Emmett-Teller (BET) adsorption isotherms [46].

The maximum adsorption capacity was calculated as 1,000 mg/g from the Langmuir isotherm model. The experimental capacity (950 mg/g, Fig. 6d) is quite close to this value. In Table 2, the analogy of the adsorption capacities and experimental conditions of some adsorbents in the literature can be seen. It was clear that the green walnut hulls provided the highest adsorption capacity of all.

3.6. Kinetic studies and investigation of agitation time

The investigation of the optimum agitation time was executed for 5, 15, 30, 60, 120, 300, and 1,440 min at 25°C. The adsorption rate was very rapid, even in the first 5 min, and the removal efficiency was calculated to be 79.13 ± 0.75%. This result presumably was a sign of having a large number of active adsorption sites. When the existing adsorption sites were occupied, the adsorption efficiency remained constant [52]. Then, the highest value was reached at 1,440 min with 92.60 ± 1.15% of removal efficiency.

Kinetic models were investigated to get information on the design and modeling of the removal processes. The kinetic studies were researched by examining the Lagergren pseudo-first-order, pseudo-second-order, and Weber–Morris's models. The data obtained from the above-mentioned kinetic models and the related equations are tabulated in Fig. 7 and Table 3.

Table 2
Comparison of agriculturally based adsorbents for MB removal with respect to some experimental conditions and adsorption capacities

Adsorbent	Optimum pH	Agitation time (min)	Adsorbent dose (g/L)	Maximum adsorption capacity (mg/g)	References
Parsley stalks	7–10	240	2	400	[6]
Cucumber peel	7–10	100	2	111.11	[6]
Watermelon seed hulls	7–10	80	2	57.14	[6]
Beetroot functionalized pumpkin peel activated carbon	7	180	5	198.15	[38]
Silica coated soya waste	6	15	2	90	[47]
Raw peach shell particle	5.5	180	4	183.6	[46]
Oil palm empty fruit bunch	8.19	–	*0.05 g	185.19	[33]
Mentha plant waste biochar-700°C	10	30	1	588.24	[40]
Magnolia grandiflora tree leaves biochar	12	1,440	0.5	101.27	[50]
Mangosteen peel wastes biochar	10	160	0.5	871.49	[51]
Green walnut hulls	10	1,440	0.5	1,000	This study

*Adsorbent amount

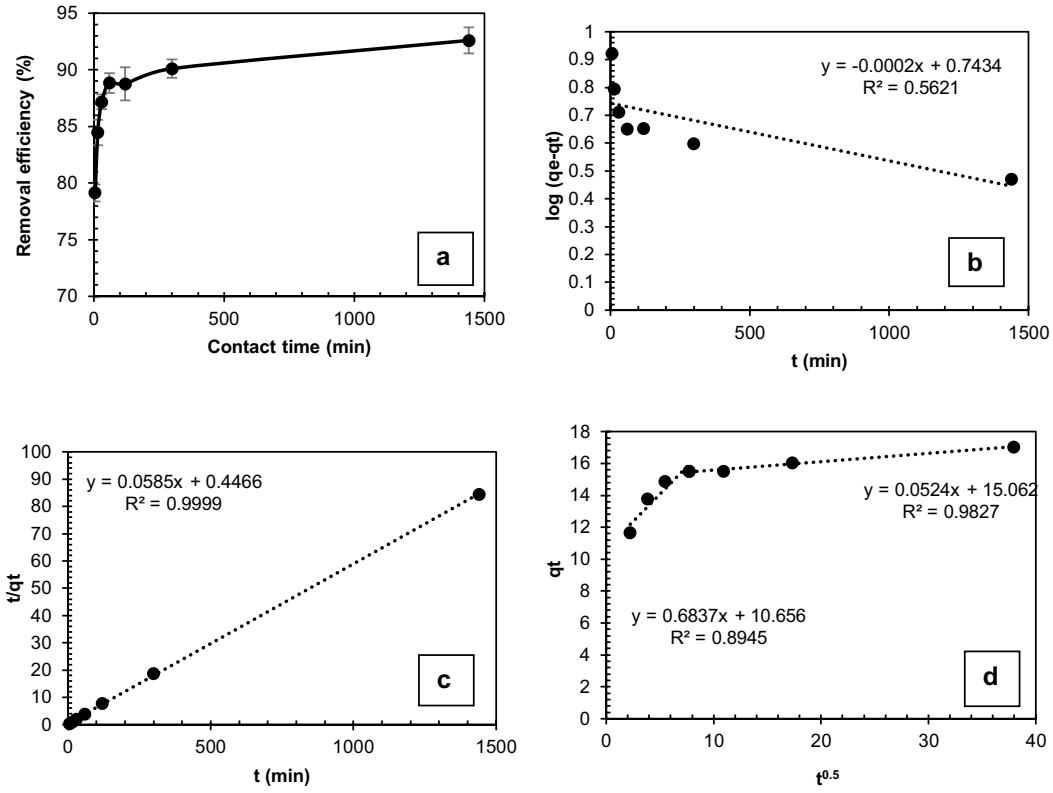

Fig. 7. Graphs of kinetic models, (a) removal efficiency vs. agitation time, (b) pseudo-first-order, (c) pseudo-second-order, and (d) Weber–Morris kinetic models (Experimental conditions: initial pH: 10, adsorbent amount: 10 mg, initial MB concentration: 20 mg/L, agitation time range: 5–1,440 min, volume of the solution: 20 mL).

As depicted in Table 3, the highest and closest correlation coefficient (R^2) to unity was obtained for the pseudo-second-order with 0.9999. Additionally, the calculated ($q_{e,cal}$) and experimental adsorption capacities ($q_{e,exp}$) also had the closest value to each other for the pseudo-second-order. These results indicated that the adsorption kinetic agreed with the pseudo-second-order, pointing out the adsorption is chemisorption based, comprising the sharing, or exchanging of electrons between the dye molecule and the adsorbent [53]. Finally, the correlation coefficients of the intraparticle diffusion model were also found to be high. That finding showed the adsorption of the MB on green

Table 3
Kinetic data for the pseudo-first-order, pseudo-second-order, and Weber–Morris for the adsorption of MB on green walnut hulls

Model	Pseudo-first-order	Pseudo-second-order	Weber–Morris	
Equation	$\log(q_e - q_t) = \log q_e - \frac{k_1 \cdot t}{2.303}$	$\frac{t}{q_t} = \frac{1}{k_2 q_e^2} + \frac{t}{q_e}$	$q_t = k_{int} \cdot t^{0.5} + I$	
Fitted model	$\log(q_e - q_t) = 0.7434 - 0.0002t$	$\frac{t}{q_t} = 0.4466 + 0.0585t$	$q_t = 0.6837 \cdot t^{0.5} + 10.656$	$q_t = 0.0524 \cdot t^{0.5} + 15.062$
R^2	0.5621	0.9999	0.8945	0.9827
Rate constant (k)	0.0004606	0.00766	0.6837	0.0524
I (mg/g)	–	–	10.656	15.062
Calculated q_e, ($q_{e,cal}$)	5.53	17.09	–	
Experimental q_e, ($q_{e,exp}$)	20	20	–	

t: the agitation time (min); q_t and q_e express the adsorption capacity at time t and at equilibrium (mg/g);
k_1 and k_2: the pseudo-first-order (1/min); pseudo-second-order rate factors (g/mg min); I: thickness of the boundary layer (mg/g), k_{int}: Weber–Morris rate constant (mg/g min$^{0.5}$).

walnut hulls was also controlled by the intraparticle diffusion model. However, since the line did not pass through the origin, the rate limiting mechanism was not merely controlled by intraparticle diffusion. The magnitude of intercept (I) defines the effect of boundary layer thickness [54]. If the magnitude of intercept is high, it means the adsorption is boundary layer controlled. In brief, both chemical sorption and intraparticle diffusion were presumed to affect the adsorption of MB on the green walnut hulls. Similar results were recorded for the following studies: the biosorption of MB on parsley stalks [6], MB and neutral red removal by soya waste [47], and MB adsorption with pumpkin peel [38].

3.7. Thermodynamic studies and investigation of temperature

The temperature reliance of the adsorption was researched in the temperature range of 291–353 K while other experimental conditions were constant (20 mg/L of initial MB concentration, 20 mL of volume, 10 mg of adsorbent amount, pH 10 and agitation time 1,440 min). The thermodynamic parameters of entropy change ($\Delta S°$), enthalpy change ($\Delta G°$), and standard Gibbs free energy ($\Delta G°$) were calculated, and the results are indicated in Table 4. $\Delta H°$ and $\Delta S°$ values were obtained by the slope and the intercept of the plot between $\ln K_L$ and $1/T$, respectively. The related equations are also represented in Table 4. The removal efficiencies were observed to insignificantly decrease as the temperature increased. The removal efficiencies were 98.54 ± 0.20%, 97.91 ± 0.99%, 97.84 ± 0.30%, 96.23 ± 0.36% at 291, 303, 333, and 353 K. The relationship between the removal efficiencies and temperature is shown in Fig. 8.

The positive value of $\Delta S°$ indicated increased randomness in the system. In addition, the $\Delta H°$ values below zero showed the adsorption was exothermic, namely as the temperature increases, the adsorption efficiency will decrease [30]. The decrease in the adsorption efficiency with increased temperature might be the reason for the weakening in adsorptive attractions between MB molecules and active binding sites of green walnut hulls [40]. The plot in Fig. 8 confirms this phenomenon. The $\Delta G°$ value below zero pointed out the spontaneous and favorable nature of the adsorption process. Similar results were reported for the MB adsorption with cucumber peels and watermelon seed hulls [6]. The thermodynamic behavior of the Cress seed mucilage magnetic composites for the MB

Table 4
The thermodynamic values for the adsorption of MB on green walnut hulls

Temperature (K)	$\Delta S°$ (J/mol K)	$\Delta H°$ (kJ/mol)	$\Delta G°$ (kJ/mol)
291	2.61	–10.99	–11.76
303			–11.79
333			–11.87
353			–11.92
Equations	$\Delta G° = -RT\ln K_L$	$\ln K_L = \frac{\Delta H°}{RT} + \frac{\Delta S°}{R}$	

T: temperature (K); $\Delta S°$: entropy changes (J/mol K); $\Delta G°$: free energy change (kJ/mol); $\Delta H°$: enthalpy changes (kJ/mol); K_L: thermodynamic equilibrium constant (L/mol); R: gas constant (8.314 J/mol K).

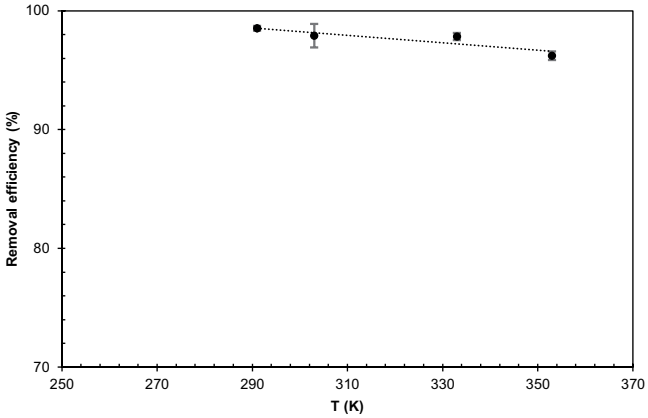

Fig. 8. The adsorption performances at various temperatures (Experimental conditions: initial pH: 10, adsorbent amount: 10 mg, initial MB concentration: 20 mg/L, agitation time: 1,440 min, volume of the solution: 20 mL)

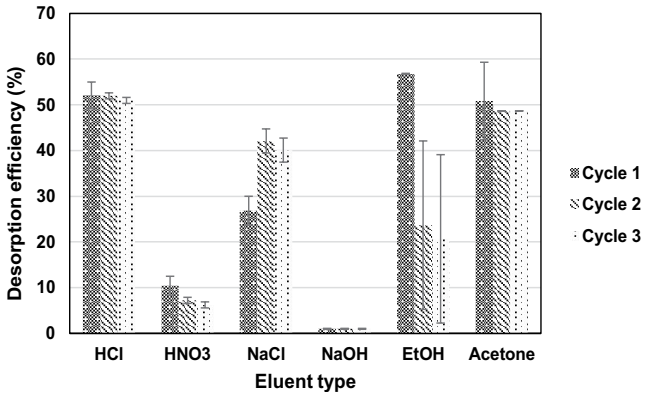

Fig. 9. Desorption of MB from the adsorbent by various solutions.

adsorption also confirmed spontaneous and exothermic behaviors [55]. On the contrary, the MB removal with parsley stalk recorded that the adsorption was endothermic, and the entropy change of the system was positive, while the $\Delta G°$ was below zero [6]. In addition, the adsorption of the MB by pumpkin peels reported an endothermic nature due to decreased viscosity, increased mobility of the analyte molecules, the activation of the adsorbent surface, and the dilation of the pore size [38].

3.8. Desorption studies

The desorption of the adsorbed methylene blue from the green walnut hulls adsorbent was investigated using HCl (1 mol/L), HNO_3 (1 mol/L), NaCl (1 mol/L), NaOH (2 mol/L), ethanol, and acetone. 20 mL of these solutions were used for the desorption process. After 24 h, to remove the excess desorption solutions, the adsorbents were washed with distilled water several times. The results are presented in Fig. 9. The desorption efficiencies were below 60%. The distilled water could not desorb the MB from the adsorbent. The highest desorption efficiencies were obtained for HCl (52.08 ± 2.92%), acetone (50.84 ± 8.47%) and the first cycle of ethanol (56.78 ± 0.11%). The low desorption efficiencies might be a result of chemically binding methylene blue molecules on the green walnut hulls adsorbent [38]. After the third cycle, the adsorption efficiencies of the adsorbents treated by NaCl, NaOH, ethanol, and acetone still were above 95%. However, with the third cycle, the adsorption efficiencies for those treated HCl and HNO_3 reached nearly 30%. This trend might be because of the deformation of the adsorbent surface by strong acids [56]. Additionally, it is thought that the high adsorption efficiency of the adsorbents studied with other desorption solutions is due to the high capacity of the adsorbent.

3.9. Analytical applications

The proposed method was applied to the real industrial wastewater effluents (WE1, WE2) and tap water samples. The samples were spiked with 10 and 100 mg/L of MB, and the adsorption process was applied under optimum experimental conditions. Blank samples were also prepared. The removal efficiencies of the 10 mg/L spiked water samples were found to be 98.21 ± 1.16%, 97.45 ± 0.94%, 99.75 ± 0.12% for WE1, WE2, and the tap water samples, respectively. Similarly, the removal efficiencies obtained in WE1, WE2, and the tap water samples with 100 mg/L MB spiked were as follows, respectively: 97.33 ± 1.52%, 96.22 ± 0.85%, and 97.04 ± 0.25%. The results indicated that the prepared adsorbent successfully removed the MB dye from the complex matrix of the studied real water samples.

4. Conclusion

In this study, it was found that green walnut hulls, which is a waste released in large quantities, successfully removed the MB from the aqueous environment. With this study, it was clearly understood that green walnut hulls are a friendly and effective option to diminish environmental pollution. As seen in the comparison chart, green walnut hulls had a huge adsorption capacity (1,000 mg/g) for MB. The optimum adsorbent dose (0.5 g/L) is much lower than that of most of the adsorbents in the literature. Although there is no special pre-treatment (chemical, and thermal activation, etc.), in the preparation of this adsorbent, it is very important that the adsorbent has a high capacity. In this way, an unnecessary use of time, chemicals, and energy is prevented. This stands out as an important advantage for the environment. The optimum pH was calculated to be 10. The adsorption process agreed with the Langmuir isotherm model with an R^2 value of 0.9816. The pseudo-second-order was defined well by the experimental data. According to the thermodynamic studies, the adsorption was exothermic, spontaneous, and feasible. Desorption was investigated by various solutions. However, desorption efficiencies were below 60%, indicating possible chemical binding. The adsorbent applied to the real water samples successfully. With this study, an easily accessible and prepared, inexpensive, environmentally friendly adsorbent has been developed for MB removal. For future research, green walnut hulls could be used for the removal of other contaminants through the application of different processes.

Funding

This research did not receive any specific grant from funding agencies in the public, commercial, or not-for-profit sectors.

Conflict of interests

The authors declare that they have no competing interests.

References

[1] J. Fu, Z. Chen, X. Wu, M. Wang, X. Wang, J. Zhang, J. Zhang, Q. Xu, Hollow poly(cyclotriphosphazene-co-phloroglucinol) microspheres: an effective and selective adsorbent for the removal of cationic dyes from aqueous solution, Chem. Eng. J., 281 (2015) 42–52.
[2] S. Shakoor, A. Nasar, Removal of methylene blue dye from artificially contaminated water using citrus limetta peel waste as a very low cost adsorbent, J. Taiwan Inst. Chem. Eng., 66 (2016) 154–163.
[3] V.K. Gupta, S. Agarwal, R. Ahmad, A. Mirza, J. Mittal, Sequestration of toxic congo red dye from aqueous solution using ecofriendly guar gum/activated carbon nanocomposite, Int. J. Biol. Macromol., 158 (2020) 1310–1318.
[4] P.M.K. Reddy, P. Verma, C. Subrahmanyam, Bio-waste derived adsorbent material for methylene blue adsorption, J. Taiwan Inst. Chem. Eng., 58 (2016) 500–508.
[5] W.-J. Luo, Q. Gao, X.-L. Wu, C.-G. Zhou, Removal of cationic dye (methylene blue) from aqueous solution by humic acid-modified expanded perlite: experiment and theory, Sep. Sci. Technol., 49 (2014) 2400–2411.
[6] G. Akkaya, F. Güzel, Application of some domestic wastes as new low-cost biosorbents for removal of methylene blue: kinetic and equilibrium studies, Chem. Eng. Commun., 201 (2014) 557–578.
[7] A.H. Hashem, E. Saied, M.S. Hasanin, Green and ecofriendly bio-removal of methylene blue dye from aqueous solution using biologically activated banana peel waste, Sustainable Chem. Pharm., 18 (2020) 100333, doi: 10.1016/j.scp.2020.100333.
[8] C. Arora, P. Kumar, S. Soni, J. Mittal, A. Mittal, B. Singh, Efficient removal of malachite green dye from aqueous solution using *Curcuma caesia* based activated carbon, Desal. Water Treat., 195 (2020) 341–352.
[9] J. Mittal, Permissible synthetic food dyes in India, Resonance, 25 (2020) 567–577.
[10] V. Katheresan, J. Kansedo, S.Y. Lau, Efficiency of various recent wastewater dye removal methods – a review, J. Environ. Chem. Eng., 6 (2018) 4676–4697.
[11] I. Anastopoulos, G.Z. Kyzas, Agricultural peels for dye adsorption: a review of recent literature, J. Mol. Liq., 200 (2014) 381–389.
[12] J. Mittal, A. Mariyam, F. Sakina, R.T. Baker, A.K. Sharma, A. Mittal, Batch and bulk adsorptive removal of anionic dye using metal/halide-free ordered mesoporous carbon as adsorbent, J. Cleaner Prod., 321 (2021) 129060, doi: 10.1016/j.jclepro.2021.129060.
[13] E. Santoso, R. Ediati, Y. Kusumawati, H. Bahruji, D.O. Sulistiono, D. Prasetyoko, Review on recent advances of carbon based adsorbent for methylene blue removal from waste water, Mater. Today Chem., 16 (2020) 100233, doi: 10.1016/j.mtchem.2019.100233.
[14] J. Mittal, R. Ahmad, M.O. Ejaz, A. Mariyam, A. Mittal, A novel, eco-friendly bio-nanocomposite (Alg-Cst/Kal) for the adsorptive removal of crystal violet dye from its aqueous solutions, Int. J. Phytorem., (2021) 1–12, doi: 10.1080/15226514.2021.1977778.
[15] A. Mariyam, J. Mittal, F. Sakina, R.T. Baker, A.K. Sharma, A. Mittal, Efficient batch and fixed-bed sequestration of a basic dye using a novel variant of ordered mesoporous carbon as adsorbent, Arabian J. Chem., 14 (2021) 103186, doi: 10.1016/j.arabjc.2021.103186.
[16] J. Mittal, Recent progress in the synthesis of layered double hydroxides and their application for the adsorptive removal of dyes: a review, J. Environ. Manage., 295 (2021) 113017, doi: 10.1016/j.jenvman.2021.113017.
[17] I. Ghosh, S. Kar, T. Chatterjee, N. Bar, S.K. Das, Removal of methylene blue from aqueous solution using *Lathyrus sativus* husk: adsorption study, MPR and ANN modelling, Process Saf. Environ. Prot., 149 (2021) 345–361.
[18] T.M. Dao, T. Le Luu, Synthesis of activated carbon from macadamia nutshells activated by H_2SO_4 and K_2CO_3 for methylene blue removal in water, Bioresour. Technol. Rep., 12 (2020) 100583, doi: 10.1016/j.biteb.2020.100583.
[19] R. Subramaniam, S. Kumar Ponnusamy, Novel adsorbent from agricultural waste (cashew nut shell) for methylene blue dye removal: optimization by response surface methodology, Water Resour. Ind., 11 (2015) 64–70.
[20] J.-E. Ali, A. Ostadrahimi, M. Tabibiazar, R. Amarowicz, A comprehensive review on the chemical constituents and functional uses of walnut (*Juglans* spp.) husk, Int. J. Mol. Sci., 20 (2019) 3920, doi: 10.3390/ijms20163920.
[21] A. Çelekli, S.S. Birecikligil, F. Geyik, H. Bozkurt, Prediction of removal efficiency of Lanaset Red G on walnut husk using artificial neural network model, Bioresour. Technol., 103 (2012) 64–70.
[22] H. Godini, F. Hashemi, L. Mansuri, M. Sardar, G. Hassani, S.M. Mohseni, A.A. Alinejad, S. Golmohammadi, A. Sheikh Mohammadi, Water polishing of phenol by walnut green hull as adsorbent: an insight of adsorption isotherm and kinetic, J. Water Reuse Desalin., 6 (2016) 544–552.
[23] A. Çelekli, H. Bozkurt, F. Geyik, Artificial neural network and genetic algorithms for modeling of removal of an azo dye on walnut husk, Desal. Water Treat., 57 (2016) 15580–15591.
[24] X.S. Wang, Z.Z. Li, C. Sun, A comparative study of removal of Cu(II) from aqueous solutions by locally low-cost materials: marine macroalgae and agricultural by-products, Desalination, 235 (2009) 146–159.
[25] X.S. Wang, Z.Z. Li, S.R. Tao, Removal of chromium(VI) from aqueous solution using walnut hull, J. Environ. Manage., 90 (2009) 721–729.
[26] N. Dalali, A. Hagghi, Removal of cadmium from aqueous solutions by walnut green husk as a low-cost biosorbent, Desal. Water Treat., 57 (2016) 13782–13794.
[27] M.R.M. Shafiee, M. Sadeghian, M. Kargar, $ZnFe_2O_4$-Fe_2O_3-CeO_2 composite nanopowder: preparation, magnetic properties, and 4-chlorophenol removal characterizations, Ceram. Int., 43 (2017) 14068–14073.
[28] A. Safinejad, M.A. Chamjangali, N. Goudarzi, G. Bagherian, Synthesis and characterization of a new magnetic bio-adsorbent using walnut shell powder and its application in ultrasonic assisted removal of lead, J. Environ. Chem. Eng., 5 (2017) 1429–1437.
[29] X. Li, Y. Tang, X. Cao, D. Lu, F. Luo, W. Shao, Preparation and evaluation of orange peel cellulose adsorbents for effective removal of cadmium, zinc, cobalt and nickel, Colloids Surf., A, 317 (2008) 512–521.
[30] C.-S. Zhu, L.-P. Wang, W. Chen, Removal of Cu(II) from aqueous solution by agricultural by-product: peanut hull, J. Hazard. Mater., 168 (2009) 739–746.
[31] J. Li, Q. Lin, X. Zhang, Y. Yan, Kinetic parameters and mechanisms of the batch biosorption of Cr(VI) and Cr(III) onto *Leersia hexandra* swartz biomass, J. Colloid Interface Sci., 333 (2009) 71–77.
[32] S. Hajialigol, S. Masoum, Optimization of biosorption potential of nano biomass derived from walnut shell for the removal of Malachite Green from liquids solution: experimental design approaches, J. Mol. Liq., 286 (2019) 110904, doi: 10.1016/j.molliq.2019.110904.
[33] C.Y. Ng, Y.Y. Tan, A.C.K. Mun, L.Y. Ng, Comparison study of adsorbent produced from renewable resources: oil palm empty fruit bunch and rice husk, Mater. Today:. Proc., 29 (2020) 149–155.
[34] D.C.C. da Silva, J.M.T. de A. Pietrobelli, Residual biomass of chia seeds (*Salvia hispanica*) oil extraction as low cost and

eco-friendly biosorbent for effective reactive yellow B2R textile dye removal: characterization, kinetic, thermodynamic and isotherm studies, J. Environ. Chem. Eng., 7 (2019) 103008, doi: 10.1016/j.jece.2019.103008.
[35] W. Cherdchoo, S. Nithettham, J. Charoenpanich, Removal of Cr(VI) from synthetic wastewater by adsorption onto coffee ground and mixed waste tea, Chemosphere, 221 (2019) 758–767.
[36] E. Alver, A.Ü. Metin, F. Brouers, Methylene blue adsorption on magnetic alginate/rice husk bio-composite, Int. J. Biol. Macromol., 154 (2020) 104–113.
[37] I. Ullah, R. Nadeem, M. Iqbal, Q. Manzoor, Biosorption of chromium onto native and immobilized sugarcane bagasse waste biomass, Ecol. Eng., 60 (2013) 99–107.
[38] J. Rashid, F. Tehreem, A. Rehman, R. Kumar, Synthesis using natural functionalization of activated carbon from pumpkin peels for decolourization of aqueous methylene blue, Sci. Total Environ., 671 (2019) 369–376.
[39] Y. Ren, C. Cui, P. Wang, Pomelo peel modified with citrate as a sustainable adsorbent for removal of methylene blue from aqueous solution, Molecules, 23 (2018) 1342, doi: 10.3390/molecules23061342.
[40] A.P. Rawat, V. Kumar, D.P. Singh, A combined effect of adsorption and reduction potential of biochar derived from Mentha plant waste on removal of methylene blue dye from aqueous solution, Sep. Sci. Technol., 55 (2020) 907–921.
[41] J. Benvenuti, A. Fisch, J.H.Z. dos Santos, M. Gutterres, Silica-based adsorbent material with grape bagasse encapsulated by the sol-gel method for the adsorption of Basic Blue 41 dye, J. Environ. Chem. Eng., 7 (2019) 103342, doi: 10.1016/j.jece.2019.103342.
[42] M. Ahmaruzzaman, Industrial wastes as low-cost potential adsorbents for the treatment of wastewater laden with heavy metals, Adv. Colloid Interface Sci., 166 (2011) 36–59.
[43] X. Zheng, H. Zheng, Z. Xiong, R. Zhao, Y. Liu, C. Zhao, C. Zheng, Novel anionic polyacrylamide-modify-chitosan magnetic composite nanoparticles with excellent adsorption capacity for cationic dyes and pH-independent adsorption capability for metal ions, Chem. Eng. J., 392 (2020) 123706, doi: 10.1016/j.cej.2019.123706.
[44] S. He, Y. Li, L. Weng, J. Wang, J. He, Y. Liu, K. Zhang, Q. Wu, Y. Zhang, Z. Zhang, Competitive adsorption of Cd^{2+}, Pb^{2+} and Ni^{2+} onto Fe^{3+}-modified argillaceous limestone: Influence of pH, ionic strength and natural organic matters, Sci. Total Environ., 637–638 (2018) 69–78.
[45] M.K. Seliem, M. Barczak, I. Anastopoulos, D.A. Giannakoudakis, A novel nanocomposite of activated serpentine mineral decorated with magnetic nanoparticles for rapid and effective adsorption of hazardous cationic dyes: kinetics and equilibrium studies, Nanomaterials, 10 (2020) 684, doi: 10.3390/nano10040684.
[46] S. Marković, A. Stanković, Z. Lopičić, S. Lazarević, M. Stojanović, D. Uskoković, Application of raw peach shell particles for removal of methylene blue, J. Environ. Chem. Eng., 3 (2015) 716–724.
[47] A. Batool, S. Valiyaveettil, Chemical transformation of soya waste into stable adsorbent for enhanced removal of methylene blue and neutral red from water, J. Environ. Chem. Eng., 9 (2021) 104902, doi: 10.1016/j.jece.2020.104902.
[48] N. Nasseh, L. Taghavi, B. Barikbin, A.R. Harifi-Mood, The removal of Cr(VI) from aqueous solution by almond green hull waste material: kinetic and equilibrium studies, J. Water Reuse Desalin., 7 (2017) 449–460.
[49] S. Hong, C. Wen, J. He, F. Gan, Y.-S. Ho, Adsorption thermodynamics of methylene blue onto bentonite, J. Hazard. Mater., 167 (2009) 630–633.
[50] B. Ji, J. Wang, H. Song, W. Chen, Removal of methylene blue from aqueous solutions using biochar derived from a fallen leaf by slow pyrolysis: behavior and mechanism, J. Environ. Chem. Eng., 7 (2019) 103036, doi: 10.1016/j.jece.2019.103036.
[51] Z. Zhang, L. Xu, Y. Liu, R. Feng, T. Zou, Y. Zhang, Y. Kang, P. Zhou, Efficient removal of methylene blue using the mesoporous activated carbon obtained from mangosteen peel wastes: kinetic, equilibrium, and thermodynamic studies, Microporous Mesoporous Mater., 315 (2021) 110904, doi: 10.1016/j.micromeso.2021.110904.
[52] N. Nasseh, I. Nasseh, M. Khodadadi, A. Beirami, M. Kamranifar, The removal of lead from aqueous solution using almond green hull (*Prunus amygdalus-Fascionello*) waste material magnetized with Fe_3O_4, Ann. Military Health Sci. Res., 15 (2017) 66336, doi: 10.5812/amh.66336.
[53] A. Ahmadpour, M. Tahmasbi, T.R. Bastami, J.A. Besharati, Rapid removal of cobalt ion from aqueous solutions by almond green hull, J. Hazard. Mater., 166 (2009) 925–930.
[54] G. Moussavi, B. Barikbin, Biosorption of chromium(VI) from industrial wastewater onto pistachio hull waste biomass, Chem. Eng. J., 162 (2010) 893–900.
[55] A. Allafchian, Z.S. Mousavi, S.S. Hosseini, Application of cress seed musilage magnetic nanocomposites for removal of methylene blue dye from water, Int. J. Biol. Macromol., 136 (2019) 199–208.
[56] M. Ajmal, R.A.K. Rao, M.A. Khan, Adsorption of copper from aqueous solution on *Brassica cumpestris* (mustard oil cake), J. Hazard. Mater., 122 (2005) 177–183.